EXPLOSIONS IN OFFSHORE MODULES

Bjørn H. Hjertager
Telemark Institute of Technology (SiT) and
Telemark Innovation Centre (Tel-Tek)
Kjølnes, N-3900 PORSGRUNN, NORWAY

Gas explosion hazard assesments in offshore gas handling operations are crucial to obtain an acceptable level of safety. In order to perform such assesments good predictive tools are needed, which take account of the relevant parameters, such as geometrical design variables and gas cloud type and distribution. A theoretical simulation model must therefore be tested against sufficient experimental data prior to becoming a useful tool. Experimental data relevant to offshore module explosions will be presented. Numerical prediction methods capable of predicting flame and pressure development in turbulent gas explosions are also presented. Special attention is given to methods which adopt the k-ϵ model of turbulence and the eddy-dissipation model of turbulent combustion. Several simulation cases related to offshore situations will be presented and comparisons will be made with experimental data as well as data from real accidents.
(Keywords: Combustion, Deflagration, Turbulence, Explosion, Offshore, Platforms)

1. INTRODUCTION

1.1 The problem

Gas explosion hazard assessment in flammable gas handling operations is crucial in obtaining an acceptable level of safety. In order to perform such assessments, good predictive tools are needed. These tools should take account of relevant parameters, such as geometrical design variables and gas cloud distribution. A theoretical model must therefore be tested against sufficient experimental data prior to becoming a useful tool. The experimental data should include variations in geometry as well as gas cloud composition and the model should give reasonable predictions without use of geometry or case-dependent constants.

1.2 Relevant works

It has in the past been usual to predict the flame and pressure development in vented volumes by modeling the burning velocity of the propagating flame. This may be succesful if we have a simple mode of flame propagation such as axial, cylindrical or spherical propagation in volumes without obstructions in the flow. If these are present, however, it is almost impossible to track the flame front throughout complex geometries. It has been apparent that in these situations it is more useful to model the

propagation by calculating the rate of fuel combustion at different positions in the flammable volume. It is also important to have a model which is able to model both subsonic and supersonic flame propagation to enable a true prediction of what can happen in an accident scenario. One such model which in principle meets all these needs has been proposed by Hjertager (1,2). The model has been tested against experimental data from various homogeneous stoichiometric fuel-air mixtures in both large- and small-scale geometries.

1.3 Objectives

The present paper will review the status of knowledge of flame and pressure development in gas explosions relevant to offshore modules. Both experimental and theoretical results are discussed.

2. GOVERNING EQUATIONS

2.1 Mass and momentum

The problem of turbulent explosion can be handled by solving for the time-mean evolution of time-mean values of the dependent variables in the domain of interest. The time-mean of a variable varying with time, t, may be expressed as:

$$\Phi(t) = \frac{1}{T}\int_{t}^{t+T} \varphi(\tau)\, d\tau \qquad (1)$$

where $\Phi(t)$ is the time-mean of the instantaneous value $\phi(t)$ averaged over the time interval T. T must satisfy two competing demands. Firstly, it must be small enough not to smear out the sought time dependence of the system under consideration. Secondly, it must be large enough to be able to produce sufficient information to enable relevant time-mean values in the interval. This means that time-mean values of both the relevant variables and their second order correlations must be obtainable in the time interval T. This is often possible since conversely, turbulence has higher frequencies than the large-scale motion which generates turbulence. The equations of motion and the energy equation can thus be expressed in tensor notation as:

$$\frac{\partial}{\partial t}\rho + \frac{\partial}{\partial x_j}(\rho U_j) = 0 \qquad (2)$$

$$\frac{\partial}{\partial t}(\rho U_i) + \frac{\partial}{\partial x_j}(\rho U_j U_i) = -\frac{\partial p}{\partial x_i} + \frac{\partial}{\partial x_j}(\sigma_{ij}) + \rho g_i \qquad (3)$$

$$\frac{\partial}{\partial t}(\rho h) + \frac{\partial}{\partial x_j}(\rho U_j h) = -\frac{\partial}{\partial x_j}(J_{h,j}) + \frac{Dp}{Dt} + S_h \qquad (4)$$

Here U_i is the velocity component in the x_i coordinate direction; p is the pressure, ρ is the density; h is the enthalpy; σ_{ij} and $J_{h,j}$ are the turbulent fluxes of momentum and energy; g_i is the gravitational acceleration in the x_i-direction and S_h is the additional source term for enthalpy.

2.2 Chemical species

The combustion is treated as a single step irreversible chemical reaction with finite reaction rate between fuel and oxygen. Hence, the reaction scheme may be written as:

$$1 \text{ kg fuel} + s \text{ kg oxygen} \rightarrow (1+s) \text{ kg products} \qquad (5)$$

Here s is the stoichiometric oxygen requirement to burn 1 kg of fuel. This simple reaction scheme results in mixture composition being determined by solving for only two variables, namely mass fraction of fuel, m_{fu}, and the mixture fraction, f.

$$\frac{\partial}{\partial t}(\rho m_{fu}) + \frac{\partial}{\partial x_j}(\rho U_j m_{fu}) = -\frac{\partial}{\partial x_j}(J_{fu,j}) + R_{fu} \qquad (6)$$

$$\frac{\partial}{\partial t}(\rho f) + \frac{\partial}{\partial x_j}(\rho U_j f) = -\frac{\partial}{\partial x_j}(J_f) \qquad (7)$$

Here R_{fu} is the time mean rate of combustion of fuel, whereas $J_{fu,j}$ and $J_{f,j}$ are the diffusive fluxes in the x_j direction. The basis for this to be valid is that the Schmidt numbers are equal for all species, an approximation which is often found in turbulent flows.
The mixture fraction is defined as:

$$f = \frac{\beta - \beta_\infty}{\beta_o - \beta_\infty} \qquad (8)$$

where ß is a conserved combined variable of, for example, mass fraction of fuel, m_{fu} and mass fraction of oxygen, m_{O2}, expressed as:

$$\beta = m_{fu} - \frac{m_{O_2}}{s} \qquad (9)$$

$ß_o$ is the value of ß at a fuel rich reference point, for example a fuel leakage point in the domain, and $ß_\infty$ is the value of ß at an oxygen rich reference point, for example the ambient air condition. For a homogeneous premixed system the mixture fraction will be constant in the domain of interest and consequently only the m_{fu} equation needs to be solved.

3. TURBULENCE AND COMBUSTION MODELS

3.1 General

To solve the governing equations (2), (3), (4), (6) and (7) given above the fluxes, σ_{ij} and $J_{\Phi,j}$, and the rate of combustion, R_{fu}, have to be modelled together with specification of relevant boundry conditions. Both the fluxes and the combustion rate are time-mean averaged values of fluctuating quantities. The fluxes can, for a general variable, Φ, and a velocity component U_j, be expressed as:

$$J_{\phi,j}=-\rho\overline{u_j\varphi} \tag{10}$$

and

$$\sigma_{ij}=-\rho\overline{u_i u_j} \tag{11}$$

where u_i and ϕ are the instantaneous fluctuations around the time-mean values U_i and Φ, respectively. The overbar indicates time-mean value over the time interval T as defined in expression 1. When modelling the correlations given in (10) and (11) it is usual to relate these to the product of time mean gradients of the relevant variables and an effective turbulent transport coefficient. For a general scalar variable Φ and a velocity component U_j the relations are:

$$J_{\phi,j}=-\frac{\mu_{eff}}{\sigma_\phi}\frac{\partial\phi}{\partial x_j} \tag{12}$$

and

$$\sigma_{ij}=\mu_{eff}\left(\frac{\partial U_i}{\partial x_j}+\frac{\partial U_j}{\partial x_i}\right)-\frac{2}{3}\delta_{ij}\left(\rho k+\mu_{eff}\frac{\partial U_k}{\partial x_k}\right) \tag{13}$$

respectively.

Here δ_{ij} = 1 if i=j and δ_{ij} = 0 if i≠j. An effective viscosity μ_{eff} and the kinetic energy of turbulence have been introduced in the above expressions, together with an effective Prandtl/Schmidt number σ_ϕ. The kinetic energy of turbulence, k, is related to the fluctuating turbulence velocity components in the three coordinate directions as:

$$k=\frac{1}{2}\left(\overline{u_1^2}+\overline{u_2^2}+\overline{u_3^2}\right) \tag{14}$$

The effective turbulence viscosity is given by two turbulence parameters, the isotropic turbulence velocity u_t and a length scale, l, as:

$$\mu_{eff}=\mu_l+\rho u_t l \tag{15}$$

μ_l is the molecular viscosity. The determination of the turbulence velocity and length scale are done by use of a turbulence model.

3.2 Two-parameter turbulence model

The determination of u_t and l are done by application of the so-called k-ε model of turbulence given by Launder and Spalding (3). The turbulence velocity is related to the kinetic energy of turbulence, k, as:

$$u_t=\sqrt{\frac{2}{3}k} \tag{16}$$

and the length scale, l, is related to the kinetic energy of turbulence, k, and its rate of dissipation ϵ, as:

$$l\sim\frac{k^{\frac{3}{2}}}{\epsilon} \tag{17}$$

Inserting (16) and (17) into expression (15) give as result:

$$\mu_{eff}=\mu_l+C_\mu\rho\frac{k^2}{\epsilon} \tag{18}$$

C_μ is a constant taken to be 0.09 (Launder and Spalding (3)). The conservation equations that determine the distribution of k and ϵ read:

$$\frac{\partial}{\partial t}(\rho k)+\frac{\partial}{\partial x_j}(\rho U_j k)=\frac{\partial}{\partial x_j}\left(\frac{\mu_{eff}}{\sigma_k}\frac{\partial k}{\partial x_j}\right)+G-\rho\epsilon \tag{19}$$

$$\frac{\partial}{\partial t}(\rho\epsilon)+\frac{\partial}{\partial x_j}(\rho U_j\epsilon)=\frac{\partial}{\partial x_j}\left(\frac{\mu_{eff}}{\sigma_\epsilon}\frac{\partial\epsilon}{\partial x_j}\right)+C_1\frac{\epsilon}{k}G-C_2\rho\frac{\epsilon^2}{k} \tag{20}$$

The two new constants appearing above C_1 and C_2, are given the values 1.44 and 1.79, respectively. The Schmidt numbers σ_k and σ_ϵ are given the values 1.0 and 1.3, respectively, whereas the other Schmidt/ Prandtl numbers are put equal to 0.7. The generation rate of turbulence is given by:

$$G=\sigma_{ij}\frac{\partial U_j}{\partial x_i} \tag{21}$$

These production terms take account of turbulence produced by shear and compression/expansion. If buoyancy production or Rayleigh-Taylor instability production is important additional terms may be added.

3.3 Rate of combustion

The rate of combustion may be modelled according to the 'eddy-dissipation' concept by Magnussen and Hjertager (4) with the ignition/extinction modification introduced by Hjertager (5) and the quasi-laminar combustion modification introduced by Bakke and Hjertager (6). If the local turbulent Reynolds number, based on the turbulent velocity and length scale, is less than a critical value the rate of combustion is calculated according to:

$$R_{fu}=-A_{lam}n_t\frac{S_{lam}}{\delta_f}\rho m_{lim} \tag{22}$$

Here n_t is the enhancement factor related to the wrinkling of the laminar flame and this factor is proporsional to the radius of flame propagation up to a maximum radius of 0.5 m. The enhancement factor is 1.0 for a radius of 0 m and is 2.5 for radii larger than 0.5 m. S_{lam} and δ_f are the laminar burning velocity and thickness of the laminar flame. A_{lam} is a contant.

If the local turbulent Reynolds number is larger than the critical value the rate of combustion is calculated according to the eddy dissipation approach modified by the extinction/ignition criteria.

Two time scales are defined, namely the turbulent eddy mixing time scale, $\tau_e = k/\epsilon$, and the chemical time scale:

$$\tau_{ch}=A_{ch}\exp\left(\frac{E}{RT}\right)(\rho m_{fu})^{a}(\rho m_{O_2})^{b} \qquad (23)$$

Also, an ignition/extinction criterion is defined when the two time scales are in a certain ratio $(\tau_{ch} / \tau_e)^* = D_{ie}$. The rate of combustion is thus calculated as:

$$R_{fu}=0 \ldots\ldots when \frac{\tau_{ch}}{\tau_e} > D_{ie}$$

$$R_{fu}=-\frac{A}{\tau_e}\rho m_{lim} \ldots\ldots when \frac{\tau_{ch}}{\tau_e} < D_{ie} \qquad (24)$$

where m_{lim} is the smallest of three mass fractions, namely fuel, m_{fu}, oxygen m_{02}/s, or mass fraction of fuel already burnt, $m_{fu,b}$. A and D_{ie} are two constants.

4. MODELING OF COMPLEX GEOMETRIES

All geometries found in industrial practice may contain a lot of geometrical details which can influence the process to be simulated. Examples of such geometries are heat exchangers with thousands of tubes and several baffles, and regenerators with many internal heat absorbing obstructions etc. In the present context the geometries found inside modules on offshore oil and gas producing platforms constitute relevant examples of the complex geometries at hand. There are at least two routes for describing such geometries. First, we may choose to model every detail by use of very fine geomtrical resolution, or secondly we may describe the geometry by use of some suitable bulk parameters. Detailed description will always need large computer resources both with regard to memory and calculation speed. It is not feasible with present or even future computers to implement the detailed method for solving such problems. We are therefore forced to use the second line of approach, which incorporates the so-called porosity/distributed resistance (PDR) formulation of the governing equations. This method was proposed by Patankar and Spalding (7) and has been applied to analysis of heat exchangers, regenerators and nuclear reactors. Sha et al (8)

have extended the method to include advanced turbulence modeling.

The presence of geometrical details modifies the governing equations in two ways. First, only part of the total volume is available to flow and secondly solid objects offer additional resistance to the flow and additional mixing in the flow. The modified equations for use in high density geometries may be expressed by:

$$\frac{\partial}{\partial t}(\beta_v \rho \phi) + \frac{\partial}{\partial x_i}(\beta_i \rho U_i \phi) = \frac{\partial}{\partial x_i}[\beta_i \Gamma_\phi \frac{\partial \phi}{\partial x_i}] + \beta_v (S_\phi + R_\phi) \quad (25)$$

Here Φ denotes a general variable that includes the variables: U_i, h, m_{fu}, f, k and ϵ. β_v is the volume fraction occupied by the fluid, β_i is the area fraction available for flow in the x_i-direction and R_ϕ is the additional resistance or additional mixing or heat transfer caused by solid obstructions in the flow. All the volume/area fractions (porosities) may take values between 0.0, completely blocked, or 1.0, completely open. Some R_ϕ functions may be found in the report by Sha and Launder (9). These functions depend on parameters like velocity, porosity, typical dimension, pitch between obstacles, obstacle shape and orientation.

5. SOLUTION PROCEDURE

It is noted that all conservation equations have the same general form as indicated in equation (25). Solution of these equations is performed by finite-volume methods. Details of the computation method are given by Hjertager (1). Only a brief description of the solution method is given here.

The calculation domain is divided into a finite number of main grid points where the pressure p, density ρ, massfraction of fuel m_{fu}, mixture fraction f, the two turbulence quantities, k and ϵ and the volume porosity β_v, are stored. The three velocity components U, V, W and the three area porosities β_x, β_y, β_z are on the other hand, stored at grid points located midway between the main points. The conservation equations are integrated over control volumes surrounding the relevant grid points in space, and over a time interval Δt. This integration is performed using upwind differencing and implicit formulation.

The result of this is a set of non-linear algebraic equations, which are solved by application of the well known tri-diagonal matrix algorithm used along the three coordinate directions. Special care has been taken to solve the pressure/velocity/density coupling of the three momentum equations and the mass balance. The 'SIMPLE' method developed by Patankar and Spalding (10) for three-dimensional parabolic flows has been extended by Hjertager (1) to compressible flows and is used to handle this coupling. The method introduces a new variable, the socalled pressure correction which makes the necessary corrections to the velocity components, pressure and density to make them obey the mass balance constraint at the new time level. The pressure correction is determined by solving a set of algebraic equations derived from the linearized momentum equations and the mass balance.

6. EXPERIMENTAL DATA

6.1 Basic considerations

Experimental data related to off-shore platforms are scarce. In many experimental investigations it has been usual to simplify the geometry. When a flame propagates in a flammable mixture three classical modes of propagation may be identified, namely axial, cylindrical or spherical modes. In the axial mode all gas expansion following combustion gives rise to increased velocity ahead of the flame, due to the constant flow area. This situation is relevant for rooms or volumes with large length over height ratios L/D, and with openings only at either end. In the cylindrical mode the combustion generated flow ahead of the flame may be smaller due to area increase along the propagation path, i.e. the area is proportional to distance from ignition. This situation may be relevant for rooms or volumes bounded by two walls, i.e. top and bottom. The spherical mode is characterized by an area increase along the flame path which is proportional to the distance from ignition squared, thus indicating smaller velocity ahead of the flame than both axial and cylindrical modes. If the ignition source is a point source all explosions will start in the spherical mode and may subsequently be modified depending on the internal obstacle layout and on the bounding walls of the confinement.

The author has advocated a stepwise approach to establish experimental data for verification of computer models for gas explosions. Experiments were first conducted in idealised geometries to see the basic effects of obstacles and mode of flame propagation. This was done in the following geometries:

- Tube with sharp edged rings (Eckhoff et al (11); Moen et al (12) Hjertager et al (13); Hjertager et al (14) and Hjertager et al (15))
- Radial geometries with sharp and rounded obstacles (Bjørkhaug and Hjertager (16, 17, 18 and 19)
- Spherical geometries (corner) with various volume blockage ratios (Hjertager et al (20))

Following these idealised gas explosion experiments tests in real off-shore module geometries were conducted. (Hjertager et al (21))

6.2 Summary of experiments in idealised geometries

The tube, radial vessel and corner experiments demonstrated the following points:

- Peak overpressures in propane-air explosions may be two to three times higher as in methane-air explosions
- Sharp edged obstacles generate double the pressure produced by round obstacles
- A series of small obstacles cause higher explosion

pressures than a single obstacle with the same blockage ratio

- Evenly distributed venting is most effective in reducing peak pressures

- A non-homogeneous gas cloud can explode with equally great violence as a homogeneous stoichiometric mixture

- The explosion pressures in the radial geometries were two to three times lower than the corresponding pressures found in the tube geometries for the same obstacle number and blockage ratio

6.3 Offshore module experiments

Hjertager et al (21) have conducted a comprehensive series of tests using a 50 m^3 module which was 8 m long, 2.5 m high and 2.5 m wide.
The module size was a 1:5 scaled down version of typical offshore modules. Homogeneous stoichiometric clouds that covered the whole module using both methane/air and propane/air were used as test gases. Two different internal geometries equivalent to compressor and separator modules were used. Six different vent arrangements were tested which ranged from venting through all four sides to venting through louvered end walls. The vent parameter, defined as vent area A_v divided by volume, V, raised to the power 2/3, i.e. $A_v/V^{2/3}$, ranged from about 0.5 and up to about 5.0. The ignition point was also varied, either centrally in the module or close to the vent opening. In the most confined tests in the separator module (volume blockage ratio of obstructions of about 0.3), peak pressures of nearly 1 bar were found using methane/air and nearly 2 bar were found using propane/air. With increasing vent area the peak pressure decreased as shown in Figure 1.
In the compressor module tests (volume blockage ratio of 0.13) slightly lower pressures were found. Generally, no significant reduction of pressures was found when ignition was moved from the

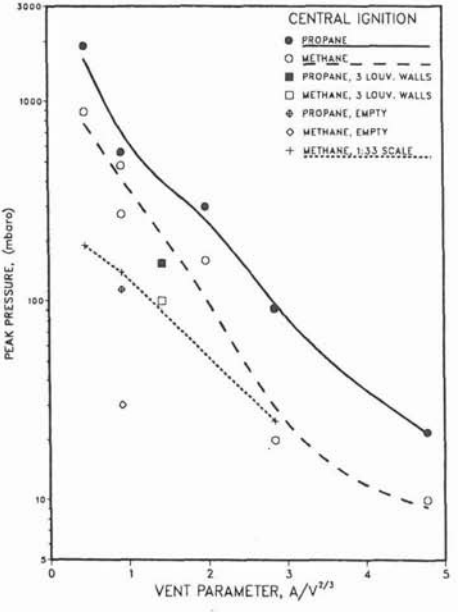

Figur 1 Peak pressure as function of vent parameter for centrally ignited explosions in the 1:5 scale separator module.

centre of the module to the vent openings. These 1:5 scale tests gave significant higher pressures when compared to the 1:33 scale tests. I.e., the 1:5 scale pressure for the most confined case was about 1 bar, whereas the corresponding pressure in 1:33 scale tests amounted to about 0.2 bar. However, when the vent area was increased the difference between the 1:5 and 1:33 scale test data deminished and for a situation with a vent parameter of about 3 the pressures were equal and amounted to about 25 mbar (See Fig.1).

Summary of venting tests. Figure 2 shows comparisons of the propane/air tests in the separator module given above, with other data collected by the author and his colleagues and others.

Det norske Veritas (22) has performed a range of explosion tests in an empty 35 m^3 module geometry using the vent size and ignition position as parameters. Their cases with rear end ignition are shown in Figure 2. It is noted that the vent parameter is much smaller (0.05-0.2) than the smallest vent parameter used in the abovementioned experiments (0.46). Because the DnV module is empty, the peak pressure versus vent parameter is, as expected, far below the present data.

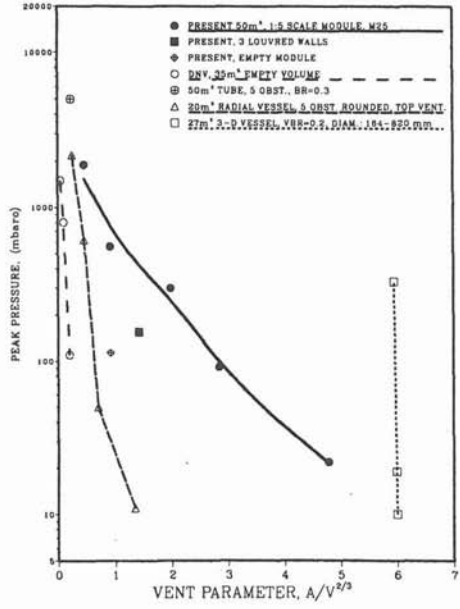

Figur 2 Peak pressures in various propane/air tests as function of the vent parameter, $A_v/V^{2/3}$.

Hjertager et al have performed a series of experiments in a 50 m^3 tube (12, 13, 14). Most of the tests in the tube have been conducted using a planar ignition source at the closed end of the tube. However, some tests using a point source have also been performed and the result of one case is shown in Figure 2. The vent parameter is somewhat smaller than in the module tests in Figure 1, but the pressure is much higher than in the module tests. In fact it seems that the tube data is a good extrapolation from the module data. This is as expected since the tube, as the module, contains obstacles.

Also shown in Figure 2 is the data from the 10m radial vessel with variable top venting (18). As we can see, the case with the smallest vent parameter, i.e. the case with solid top wall, gives

a pressure build-up that connects fairly well to the module data. However, when the top venting is increased the pressure reduction is much larger than for the module tests. This is due to the fact that the venting is evenly distributed and that ignition is very close to the top vent. Both these conditions favour a lowering of explosion pressure.

The final set of data which are shown in Figure 2 stems from the unconfined, spherical and obstructed tests performed by Hjertager et al (20). The data are collected in a 27 m^3 3-D corner, which is 1/8 of a full unconfined sphere. The vent parameter for these cases amounts to about 6.0, which is beyond the present module tests. However, it is seen that the data for a volume blockage ratio, VBR=0.2, and obstacle dimension equal 820mm and 410mm is a good extrapolation of the module data. The 3-D data also shows the large effects of obstacle size for a given VBR. As we can see the smallest obstacle dimension of 164mm and VBR=0.2 produced a peak pressure of about 0.35 bar.

7. CAPABILITIES OF GAS EXPLOSION MODEL

7.1 Idealised geometries

Hjertager (23) has given a summary of the results of calculations of some of the geometries given above using the model presented above. Some of the characteristics of the comparisons with experiments are as follows:

- The model is able to simulate the peak pressures and terminal flame speeds obtained in the large-scale tube (2.5 m diameter and 10m length) for both methane-air and propane-air with variable concentrations. Similar favourable results were found when the simulated results were compared to the experiments of Lee et al. (24). Their tests were performed in a small scale tube (5cm diameter and 3m in length) using variable concentration of hydrogen-air. The model was, however, not able to predict the transition to detonation found in the hydrogen-air experiments

- Chan et al (25) have performed a series of experiments in a channel (0.203 in heigth and 1.22m in length) with repeated obstacles and variable top venting. Bakke and Hjertager (26) have used the above model and simulated several of the test cases. The model was able to reproduce: 1) the effect variable confinement on flame speed and 2) the effect of changing position of the obstacles. Moen et al (27) have done experiments in a large-scale top vented channel (1.8m x 1.8m cross-section and 15.5m in length) using acetylene-air, propane-air and hydrogen sulphide-air mixtures. They also present simulation results using the above-mentioned model and show that the model is able to predict the difference between the three fuels. Namely, large flame acceleration in acetylene and no significant acceleration in propane and hydrogen sulphide. The model was not able to predict the transition from deflagration to detonation in acetylene-air that occur at the end of the channel.

- Bakke and Hjertager (28) have applied the model to the empty volume propane-air tests of Solberg (22). The predictions showed reasonable agreement for peak pressure versus vent area for three different volumes (3.6 litre, 35 m^3 and 425m^3).

- Bjørkhaug et al (29) used the model to analyse the experimental data from the radial vessel geometry with variable top venting. They found good correlation between model prediction and experimental data of pressure.

7.2 Module geometries

Hjertager et al (30) have incorporated the model given above into a 3D computer code and used this to simulate the module data of Hjertager et al (21) also presented above. The compressor module was modelled by using a grid of 42 x 14 x 14 points in the length, heigth and width directions, respectively. The internal equipment was modelled using approximately 100 obstructions. Figure 3 gives a summary of the simulated and measured peak pressure data in the 1:33 and 1:5 scale compressor modules. The figure shows variation of peak explosion pressures inside the module for centrally ignited clouds as function of the vent parameter. It can be noted that the predicted general trends are in good accordance with the measurements. The computer model is able to predict the following characteristics found in the experiments:

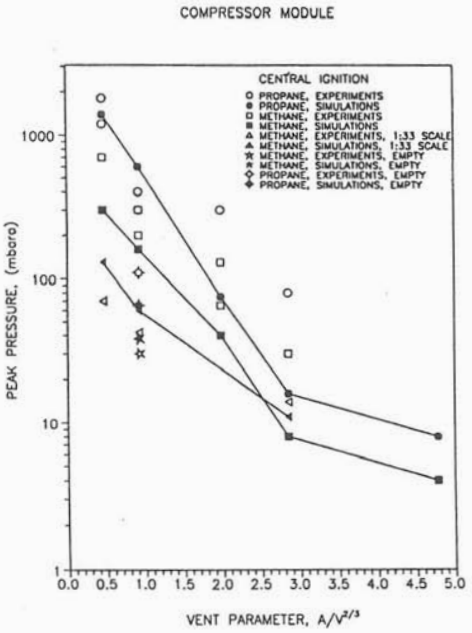

Figur 3 Peak pressure as function of vent parameter for centrally ignited explosions in the 1:5 scale compressor module - comparison beween experiments and simulations.

1) the variation of peak pressures with the vent parameter.

2) the difference between pressure build-up in methane-air and propane-air explosions.

3) the influence of two scales, i.e. 1:33 and 1:5.

4) the influence of internal process equipment on the violence of the explosion.

Although the general trends are predicted well, it is also noted that there are discrepancies between experiments and simulations. This is especially seen for the cases with vent parameters larger than about 2.0 and for the 1:5 scale methane-air test with a vent parameter of about 0.5.

7.3 Scenario calculations

Hjertager et al (31) have used the 3D gas explosion code to analyse the Piper Alpha accident. The geometrical and other data were taken from the Interim report from the Investigation of the Piper Alpha accident (32). The explosion in the module C - the compression module - was modelled using a grid of 47 x 17 x 9 points in the length, width and height directions. The internal equipment was modelled using about 55 obstructions.

Four different cases were simulated with fixed ignition point located centrally in the module, namely:

1. stoichiometric homogeneous cloud filling the whole free space

2. stoichiometric homogeneous cloud filling the right half of the free space

3. stoichiometric homogeneous cloud filling the lower half of the free space

4. stoichiometric homogeneous cloud filling one quarter of the free space located at the lower right position

The following table gives the peak pressures that were found for the four cases:

Case	Peak pressure (bar)
1	4.7
2	0.68
3	0.86
4	0.15

The table indicates a range of pressure loads from 150 mbar to 4.7 bar. The Piper Alpha report indicates that the pressures must have been larger than about 300 mbar. The model simulations indicate that three of the cases produce pressure loads larger than that. Even the case with one quarter of the module filled with flammable gas produce an explosion pressure that may produce significant damage.

8. CONCLUDING REMARKS

A summary of a computer model capable of analysing the processes which occur in turbulent gas explosions inside complex congested geometries was presented. Several computations were reported which compare the computer model against several sets of experimental data relevant for offshore situations. The agreement between predictions and measurements is in general good. However, more work is needed: 1) to develop and verify the porosity/distributed resistance model for explosion propagation in high density obstacle fields; 2) to improve the turbulent combustion model and 3) to develop a model for deflagration to detonation transition.

A summary of some experimental data related to gas explosions in offshore modules was also presented. All the results presented in the module experiments used stoichiometric homogeneous clouds that filled the whole free space inside the module. Further studies in module experiments should include the effects of fuel cloud inhomogeneity. More data are needed to enable verification of the model in high-density geometries.

9. ACKNOWLEDGEMENT

The work on gas explosions at SiT/Tel-Tek is financially supported by Shell Research Ltd.

10. REFERENCES

1. Hjertager, B.H.: Simulation of transient compressible turbulent reactive flows, Comb. Sc. and Techn., 41, pp. 159-170, 1982.

2. Hjertager, B.H.: Numerical simulation of flame and pressure development in gas explosions, SM study No. 16, University of Waterloo Press, Ontario, Canada, pp 407-426, 1982.

3. Launder, B.E. and Spalding, D.B.: The numerical computation of turbulent flows, Computer methods in applied mechanics and engineering, 3, pp 269-289, 1974.

4. Magnussen, B.F. and Hjertager, B.H.: On the mathematical modeling of turbulent combustion with special emphasis on soot formation and combustion, 16th Symp.(Int) on combustion, Combustion Institute, Pittsburgh, Pa, pp719-729, 1976.

5. Hjertager, B.H.: Numerical simulation of turbulent flame and pressure development in gas explosions, in Fuel-air explosions, SM Study No. 16, University of Waterloo press, pp 407-426, 1982.

6. Bakke, J.R and Hjertager, B.H.: Quasi-laminar/turbulent combustion modelling, real cloud generation and boundary conditions in the FLACS-ICE code, CMI No. 865402-2, Chr. Michelsen Institute, 1986. also in Bakke's dr.scient.

thesis "Numerical simulation of gas explosions in two-dimensional geometries", University of Bergen, Bergen, 1986.

7. Patankar, S.V and Spalding, D.B.: A calculation procedure for the transient and steady-state behavior of shell-and-tube heat exchangers, in Heat Exchangers: Design and Theory Sourcebook, edited by N.H. Afgan and E.V. Schlünder, McGraw-Hill, pp 155-176, 1974.

8. Sha, W.T., Yang, C.I., Kao, T.T, and Cho, S.M.; Multi-dimensional numerical modeling of heat exchangers, Journal of Heat Transfer, 104, pp 417-425, 1982.

9. Sha, W.T. and Launder, B.E.: A model for turbulent momentum and heat transport in large rod bundles, ANL-77-73, 1979.

10. Patankar, S.V. and Spalding, D.B: A calculation procedure for heat, mass and momentum transfer in three-dimensional parabolic flows, Int. J. Heat and Mass Transfer, 15, pp 1787-1806, 1972.

11. Eckhoff, R.K., Fuhre, K., Guirao, C.M. and Lee, J.H.S.: Venting of turbulent gas explosions in a 50 m^3 chamber, Fire safety journal, 8, pp 191-197, 1984.

12. Moen, I.O., Lee, J.H.S, Hjertager, B.H., Fuhre, K. and Eckhoff, R.K.: Pressure development due to turbulent flame propagation in large-scale methane-air explosions, Combustion and flame, 47, pp 31-52, 1982.

13. Hjertager, B.H., Fuhre, K., Parker, S.J. and Bakke, J.R.: Flame acceleration of propane-air in a large-scale obstructed tube, in Prog. AIAA, Vol. 94, pp 504-522, 1984.

14. Hjertager, B.H., Fuhre, K. and Bjørkhaug, M.: Concentration effects on flame acceleration by obstacles in methane-air and propane-air vented explosions, Combustion science and technoloy, 62, pp 239-256, 1988.

15. Hjertager, B.H., Bjørkhaug, M. and Fuhre, K: Explosion propagation of non-homogeneous methane-air clouds inside an obstructed 50 m^3 vented vessel, Journal of hazardous materials, 19, pp 139-153.

16. Bjørkhaug, M. and Hjertager, B.H.: The influence of obstacles on flame propagation and pressure development in a radial vessel, Chr. Michelsen Institute, CMI Report No. 823403-4, 1982, also in Bjørkhaug's PhD thesis "Flame acceleration in obstructed radial geometries", City University, London, 1986.

17. Bjørkhaug, M. and Hjertager, B.H.: The influence of obstacles on flame propagation and pressure development in a radial vessel of ten meter radius, Chr. Michelsen Institute, CMI Report No. 843403-9, 1984, also in Bjørkhaug's PhD thesis "Flame acceleration in obstructed radial geometries", City University, London, 1986.

18. Bjørkhaug, M. and Hjertager, B.H.: The influence of confinement on flame propagation and pressure development in a radial vessel, Chr. Michelsen Institute, CMI Report No. 855403-2, 1985, also in Bjørkhaug's PhD thesis "Flame acceleration in obstructed radial geometries", City University, London, 1986.

19. Bjørkhaug, M. and Hjertager, B.H.: The influence of obstacle shape, fuel composition and obstacle layout on flame propagation and pressure development in a radial vessel of ten meter radius, Chr. Michelsen Institute, CMI Report No. 865403-1, 1986, also in Bjørkhaug's PhD thesis "Flame acceleration in obstructed radial geometries", City University, London, 1986.

20. Hjertager, B.H., Fuhre, K and Bjørkhaug, M.: Spherical gas explosion experiments in a high-density obstructed 27 m^3 corner, Chr. Michelsen Institute, CMI Report No. 865403-3, 1986. Restricted circulation.

21. Hjertager, B.H., Fuhre, K. and Bjørkhaug, M.: Gas explosion experiments in 1:33 and 1:5 scale offshore separator and compressor modules using stoichiometric homogeneous fuel/air clouds, Journal of loss prevention in the process industries, 1, pp 197-205, 1988.

22. Solberg, D.M.: Gas explosion research related to safety of ships and offshore platforms, in Fuel-air explosions, Univ. of Waterloo Press, pp 787-819, 1982.

23. Hjertager, B.H.: Simulation of gas explosions, Modeling, identificaion and control, 10, pp 227-247, 1989.

24. Lee, J.H.S, Knystautas, R. and Freiman, A.: High speed turbulent deflagration and transition to detonation in H_2-air mixtures, Combustion and flame, 56, 227-239, 1984.

25. Chan, C, Moen, I.O. and Lee, J.H.S.: Influence of confinement on flame acceleration due to repeated obstacles, Combustion and flame, 49, pp 27-39, 1983.

26. Bakke, J.R. and Hjertager, B.H.: The effect of explosion venting in obstructed channels, in Modeling and simulation in engineering, Elsevier Science Publication, pp237-241, 1986.

27. Moen, I.O, Sulmistras, A., Hjertager, B.H. and Bakke, J.R.: Turbulent flame propagation and transition to detonation in large fuel-air clouds, 21st Symposium (Int.) on combustion, The Combustion Institute, pp 1617-1627, 1986.

28. Bakke, J.R. and Hjertager, B.H.: The effect of explosion venting in empty volumes, Int. Journal of numerical methods in engineering, 24, pp 129-140, 1987.

29. Bjørkhaug, M., Bakke, J.R. and Hjertager, B.H.: Calculation of gas explosion in radial geometry using FLACS-ICE-2D, Chr.Michelsen Institute, CMI Report No. 865403-4, 1986,

also in Bjøkhaug's PhD thesis "Flame acceleration in obstructed radial geometries", City University, London, 1986.

30. Hjertager, B.H., Solberg, T. and Nymoen, K.O.: Computer modeling of gas explosion propagation in offshore modules, paper to be published, 1991.

31. Hjertager, B.H., Solberg, T. and Førrisdahl, J.E.: Computer simulation of the 'Piper Alpha' gas explosion accident, paper to be published, 1991.

32. Petrie, J.R.: Piper Alpha technical investigation, Interim report, Dept of Energy, Sept. 1988.